

TABLE I
NOISE TEMPERATURE VERSUS INCIDENT POWER (DECIBELS)

	Incident Power			
	-15 dBm	-5 dBm	+5 dBm	+15 dBm*
1N21E at 100 Hz†	21	27	37	—
1N21E at 1000 Hz†	11	15	24	—
1N23C at 1000 Hz†	17	19	25	—
NE-51H at 100 Hz and 1000 Hz†	18	20	23	—
NE2 at 100 Hz and 1000 Hz†	23	21	16	11

* Only one bulb worked at +15 dBm.

† This work, measurements made at 3 GHz.

‡ Feher [5], measurements made at 9 GHz.

to the microwave carrier and used to measure noise temperatures. For any given carrier power setting, the amplitude modulation percentage was varied to find the point at which the audio signal-to-noise ratio was 10 to 1. Detector noise, measured by this known sideband power, is compared to the theoretical 290°K noise power from a blackbody source. Noise temperature is defined [4] as the equivalent noise power to the theoretical noise power ratio, and can be expressed in decibels. The minimum detectable signal was measured with 100 percent square-wave modulation; it is defined here as the carrier power at which the signal-to-noise ratio is one to one. RF oscillator, audio modulator and amplifier circuits were not a significant source of noise in these experiments.

At modulation frequencies above 10 kHz the detection efficiency of neon bulbs drops, but noise shows no frequency dependence from 20 Hz to 10 kHz. Noise output is somewhat dependent on dc current, but independent of RF power except that each bulb ceases detecting abruptly as power is increased past some characteristic value. Many bulbs stop operating at +5 dBm, the best quit at +15 dBm. About 30 NE-2 and NE-51H gas bulbs were tested. A few bad bulbs showed noise temperatures 40 dB worse than the best one. The average bulb was perhaps 5 dB worse than the best. Minimum detectable signal is -65 dBm using a 30-Hz detection bandwidth at 1000 Hz modulation frequency.

Close examination showed a correlation between the visible discharge and noise temperatures. The best bulbs had parallel electrodes. Their dc discharge was steady and the visible portion covered the whole of one electrode. The worst bulb had parallel electrodes but its discharge flickered back and forth. Intermediate bulbs had nonparallel electrodes or imperfections so that the discharge was smaller and localized. While magnetic fields of up to 10 000 gauss could improve the performance of poor bulbs by stabilizing their flicker, the best bulbs were not improved by a field. Results reported are only for the best bulbs tested.

Some crystal noise temperatures were measured using the same equipment and techniques so that systematic errors would cancel in direct comparisons with plasma detectors. Crystals were operated in a commer-

cial waveguide mount and with a low-noise audio preamplifier. Of ten specimens, the best was a Sylvania 1N21E, for which the minimum detectable signal is the same as the plasma detector's, -65 dBm with a 30-Hz bandwidth at 1000 Hz. Noise temperatures measured in this work are found in Table I where they are compared to those obtained by Feher [5]. These data show that the plasma detector is better than a crystal for 1000-Hz modulation at powers above 1 mW. For 100-Hz modulation it is always better than the best crystal.

An NE-51H bulb was tried as a detector in a low-power 3-GHz EPR spectrometer. Comparison with the best crystal detector available confirms the plasma detector's superiority when the modulation frequency is 100 Hz.

Since the desired detector must operate at higher powers than the +15 dBm of an NE-2, a war surplus 721A TR tube was converted to a plasma detector and mounted in a waveguide cavity. The gas in the original tubes [6], a mixture of H₂ and H₂O, makes an inefficient detector, so other gases were introduced while observing detector operation. Comparing He, Ne, Ar, Ne+He, Hg₂+He and air, the most efficient high-power detector was found to be pure helium at 25 mm pressure. The best operating range is 1 to 10 watts. No noise measurements have been made, but probably the noise temperature is not as good as those measured for neon bulbs. This is because the tips of the cones in 721A tubes, while blunt, are still too sharp and not uniform enough. Improvements could surely be made.

The 721A detector with helium was installed in a high-power EPR spectrometer which is used for saturation and dynamic polarization studies [7]. A phase-locked QK625 BWO supplies up to 200 watts CW to a reflection cavity. With 100-Hz modulation, signals are seen from standard paramagnetic samples. Since no signals at all can be seen with crystal detectors after necessary power attenuation to prevent burnout, plasma detectors represent considerable improvement.

DOUGLAS C. MCCAIN¹
Lawrence Radiation Lab.
Berkeley, Calif.

¹ Now with the Department of Chemistry, University of California, Santa Barbara, Calif. 93106.

REFERENCES

- [1] M. A. Lampert and A. D. White, "Microwave technique for studying discharges in gases," *Electronics Commun.*, vol. 30, p. 124, 1953.
- [2] H. A. Burroughs and A. B. Bronwell, "High-sensitivity gas tube detector," *Tele-Tech.*, vol. 11, p. 62, 1952.
- [3] N. H. Farhat, "A plasma microwave power density detector," *Proc. IEEE* (Correspondence), vol. 52, pp. 1053-1054, September 1964.
- [4] H. C. Torrey and C. A. Whitmer, *Crystal Rectifiers*, M.I.T. Rad. Lab. Ser., vol. 15. New York: McGraw-Hill, 1949.
- [5] G. Feher, "Sensitivity considerations in microwave paramagnetic resonance absorption techniques," *Bell Sys. Tech. J.*, vol. 36, p. 449, 1957.
- [6] L. D. Smullin and C. G. Montgomery, *Microwave Duplexers*, M.I.T. Rad. Lab. Ser., vol. 14. New York: McGraw-Hill, 1949.
- [7] D. C. McCain and R. J. Myers, "Spin-lattice and spin-spin relaxation times for VO²⁺ in aqueous solution," *J. Phys. Chem.*, vol. 71, p. 192, 1967.

Characteristic Impedance of Microstrip by the Method of Moments

Abstract—The "method of moments" [1] is used to calculate the capacity per unit length of a microstrip transmission line. The characteristic impedance is obtained by assuming TEM mode of propagation. The values of the impedance calculated by this method are in good agreement with the results reported by Wheeler [2] and Sobol [3].

A cross section of the microstrip transmission line analyzed here is shown in Fig. 1. The characteristic impedance of the transmission line is determined in the following manner. The potentials of the center conductor and the ground plane are assumed to be one and zero volts, respectively. The center conductor is divided into N equal subsections, ΔC , along the cross section. Assume that the charge on the center conductor is distributed over each subsection with an unknown charge density α_j .

The boundary conditions on the ground

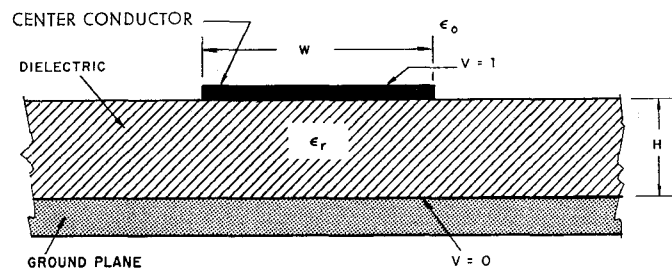


Fig. 1. Cross section of a microstrip transmission line.

TABLE I
CHARACTERISTIC IMPEDANCES OF MICROSTRIP TRANSMISSION LINES

W/H	$\epsilon_r = 6.0$		$\epsilon_r = 9.5$		$\epsilon_r = 16.0$		$\epsilon_r = 28.0$	
	Z_0^*	Z_0^\dagger	Z_0^*	Z_0^\dagger	Z_0^*	Z_0^\dagger	Z_0^*	Z_0^\dagger
0.1	135.455	134.352	110.172	110.058	85.9659	87.762	65.5298	68.819
0.2	113.272	112.255	91.809	91.776	71.6954	73.015	54.6138	57.110
0.4	91.172	89.909	73.702	73.290	57.4999	58.110	43.7391	45.281
0.7	73.613	71.995	59.379	58.502	46.2344	46.217	35.1153	35.872
1.0	62.713	60.970	50.501	49.431	39.2512	38.948	29.7629	30.144
2.0	43.149	41.510	34.592	33.493	26.7555	26.248	20.2086	20.197
4.0	27.301	26.027	21.763	20.906	16.7210	16.300	12.5529	12.474
10.0	13.341	12.485	10.568	9.981	8.0385	7.8079	5.9746	5.892

* Characteristic impedance obtained by method of moment.

† Characteristic impedance obtained by conformal mapping.

plane and at the dielectric interface are satisfied by multiple imaging. Let D_{ij} be the potential at the field point i on the center conductor due to the charge on subsection j . It is assumed that the charge is concentrated in a filament along the center of the subsection.

D_{ij} , the Green's function for this problem, may be expressed as follows.

$$D_{ij} = \frac{1}{4\pi\epsilon_r} \sum_{n=1}^{\infty} k^{2(n-1)} \ln \frac{C_{ij}^2 + (4n-2)^2}{C_{ij}^2 + (4n-4)^2} + k^{2n-1} \ln \frac{C_{ij}^2 + (4n-2)^2}{C_{ij}^2 + (4n)^2}$$

where

$$C_{ij} = \frac{\Delta C}{H} \times |2(i-1) - 2(j-1) - 1|$$

$$k = \frac{\epsilon_r - 1}{\epsilon_r + 1}$$

By enforcing the boundary condition on the center conductor, we obtain the matrix equation

$$\begin{bmatrix} D_{11} & D_{12} & \cdots & D_{1N} \\ D_{21} & D_{22} & \cdots & \\ \vdots & \vdots & \ddots & \vdots \\ D_{N1} & D_{N2} & \cdots & D_{NN} \end{bmatrix} \begin{bmatrix} \alpha_1 \\ \alpha_2 \\ \vdots \\ \alpha_N \end{bmatrix} = \begin{bmatrix} 1 \\ 1 \\ \vdots \\ 1 \end{bmatrix} \quad (1)$$

The values of the alphas in (1) are determined by matrix inversion and the capacitance per unit length is thus obtained by summing the alphas,

$$C = \sum_{j=1}^N \alpha_j \quad (\text{farads/meter}). \quad (2)$$

The characteristic impedance of the microstrip is then calculated by using the expression [4]

$$Z_0 = \frac{1}{v_0 \sqrt{C_0 C}} \quad (3)$$

where C_0 is the capacitance per unit length for the air-filled transmission line and v_0 is the speed of light.

The computer results obtained by this method for a microstrip with different dielectric constants and infinitely thin center conductor are given in Table I. For the purpose of comparison, the results for the same transmission line obtained by Sobol [3] are included in the table. The expression for the characteristic impedance of the microstrip line reported by Sobol is obtained by conformal mapping based on Wheeler's analysis [2].

The infinite series summation was terminated when the total changed by less than 10^{-4} upon addition of a term. For the results given here the center conductor was divided into 30 subsections in each case. This number was chosen by increasing the number of subsections until the resulting capacitance did not vary significantly (less than 0.1 percent).

A. FARRAR
General Electric Company
Syracuse, N. Y. 13201
A. T. ADAMS
Dept. of Elec. Engrg.
Syracuse University
Syracuse, N. Y.

REFERENCES

- [1] R. F. Harrington, *Field Computation by Moment Methods*. New York: Macmillan, 1968.
- [2] H. A. Wheeler, "Transmission-line properties of parallel strips separated by a dielectric sheet," *IEEE Trans. Microwave Theory and Techniques*, vol. MTT-13, pp. 172-185, March 1965.
- [3] H. Sobol, "Extending IC technology to microwave equipments," *Microwaves*, March 20, 1967.
- [4] H. E. Green, "The numerical solutions of some important transmission line problems," *IEEE Trans. Microwave Theory and Techniques*, vol. MTT-13, pp. 676-692, September 1965.

Guided Waves in a Class of Stripline and Other Parallel-Plate Structures

Abstract—The dominant mode of the open-sided shielded stripline is TEM and has rightly received considerable attention. Few analyses of its non-TEM properties are available. Oliner [1] and Samuilov [2] have assumed the existence of higher order modes and calculated cutoff frequencies through a transverse resonance approach. Brackelmann *et al.* [3] have made computations through series-matching, and report that non-TEM modes do not exist for open-sided shielded stripline. Bolle and Eaves [4], through a Wiener-Hopf technique, have made calculations that substantiate this. Ilgenburg and Pregla [5] have made calculations through series matching for a stripline of two strips and report H modes. However, such numerical results allow strict conclusions only for the specific parameters chosen, and, furthermore, the conclusions are subject to computational error. These practical considerations along with the aesthetic make a non-numerical investigation desirable. It will be shown that the shielded stripline, and indeed a general class of parallel-plate waveguide structures, do not support non-TEM modes.

Consider a waveguiding structure (Fig. 1) uniform in the z -direction. Between two infinite and perfectly conducting planes are N perfect conductors of arbitrary shape, surrounded by a homogeneous and isotropic dielectric. In formulating the problem of non-

Manuscript received June 2, 1969; revised July 23, 1969. This work was supported by the National Science Foundation, Grant GK-2351 and by the Advanced Research Project Agency, Contract SD-86.